Fracture Mechanics of Concrete Structures,
Proceedings FRAMCOS-2, edited by Folker H. Wittmann,
AEDIFICATIO Publishers, D-79104 Freiburg (1995)

INTERACTION OF PLURAL CRACKS IN CONCRETE DURING FLEXURAL FAILURE

H. Koide, H. Akita, and M. Tomon,
Department of Civil Engineering, Tohoku Institute of Technology, Sendai, Japan

Abstract
The behavior of plural fictitious cracks indicating fracture process zones is simulated on an unnotched plain concrete beam during a flexural failure process by finite element method (FEM) using a fictitious crack model. In experiments, four-point bending tests of displacement-control were carried out on unnotched 100 x 100 x 400 mm plain concrete beams, and the displacement rates were 0.2×10^{-6} m/s and 0.5×10^{-6} m/s at the loading point. Comparison of the experimental results and the analytical results indicates that each of the observed plural cracks corresponds to a predicted crack, the depth of which is larger than 20 mm from the concrete surface to the fictitious crack tip. Uniaxial tension tests of unnotched plain concrete specimens were also carried out to obtain a tension softening curve. From these tests, some knowledge of the most suitable test method is obtained.

1 Introduction

The interaction of plural cracks in concrete is correlated to bifurcation and localization in the fracture process. Bazant and Ohtsubo (1977) first analyzed the interaction of plural cracks in a brittle solid under thermal stresses.

Akita et al. (1992) simulated the interaction of plural cracks in concrete by applying a fictitious crack model to each of the cracks under pure bending, thermal stress and shrinkage stress, while Kurihara et al. (1994) experimentally detected plural cracks under pure bending in concrete by using many strain gages.

In this study, four-point bending tests of unnotched plain concrete beams were carried out, and plural cracks were optically observed. The interaction of the plural cracks was then simulated by FEM analysis adopting a fictitious crack model.

Uniaxial tension tests of unnotched plain concrete specimens were also carried out to obtain a tension softening curve which is used in the fictitious crack model. Petersson (1981) and Li and Shah (1994) have already presented papers on uniaxial tension tests, but either notched concrete specimens or concrete with a maximum aggregate particle size of about 10 mm were used in the tests. However, in our tests, unnotched concrete specimens with a maximum aggregate particle of 20 mm and cross section size of 80 x 80 mm were used.

2 Experimental details

2.1 Concrete

Table 1 shows the mix proportion of concrete in which ordinary portland cement was used. Compressive strength, splitting tensile strength ft, and modulus of elasticity measured on cylindrical specimens were 34 N/mm^2, 2.8 N/mm^2, and 33.4 kN/mm^2, respectively.

2.2 Uniaxial tension test

The uniaxial tension test arrangement and unnotched plain concrete specimen are shown in Fig. 1. Six specimens (T1-T6) were tested, with each having a uniform cross section size of 80 x 80 mm in the central 100 mm section ranging to a uniform 80 x 100 mm cross section for a length of 175 mm at each end. To avoid stress concentration, the profile between the uniform central and end sections varies along a circular curve as shown in Fig. 1. Four 120 mm strain gages are glued on each surface at the center of the specimen. In addition, four steel leaves are glued to the specimen around the strain gages on the front and back surfaces respectively. Strain gages display

Table 1. Mix proportion used in experiments

Water (kg/m^3)	Cement (kg/m^3)	W/C ratio(%)	Sand (kg/m^3)	Gravel (kg/m^3)	A. E. A. (g/m^3)	Max size of agg. (mm)
167	334	50	646	1, 228	86. 8	20

a slight reinforcement effect on a concrete surface. If the steel leaves aren't used, it may be difficult for a fracture process zone to develop at the central part of the specimen.

With regards to the loading control modes, load-control is first used until a set load level (below the peak load) is reached, then strain-control using a strain gage is employed until failure. Various rates of loading and strain are used on the six specimens in order to obtain a tension softening curve.

2.3 Four-point bending test

The four-point bending test arrangement and unnotched plain concrete beam specimen are shown in Fig. 2. Four specimens (B1-B4) were tested, with each specimen having a size of 100 x 100 x 400 mm. In order to reduce the frictional force, rollers are used at the loading and support points, as shown in Fig. 2. The loading points are on the lower surface in order to facilitate the observation of cracks that develop at the tensile side in the pure bending span. The loading is controlled by using one of the displacement transducers above a loading point, the rate of displacement is initially set at 0.2×10^{-6} m/s. When servo-control of the loading machine becomes impossible at this rate, the rate is changed to 0.5×10^{-6} m/s.

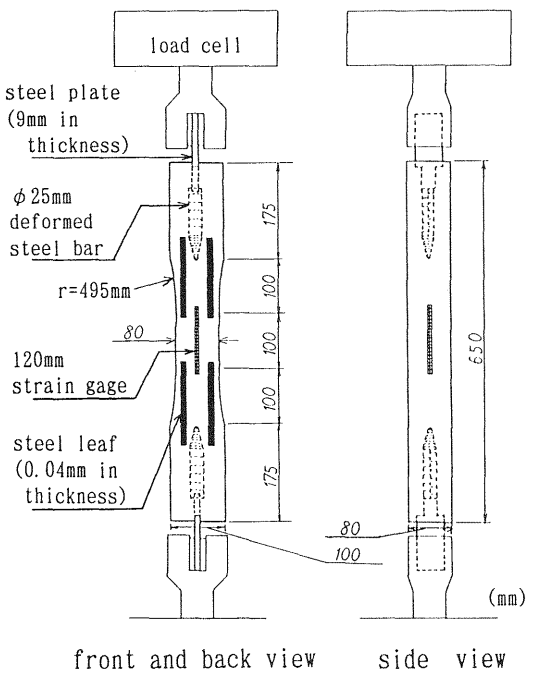

Fig. 1. Setup for uniaxial tension test

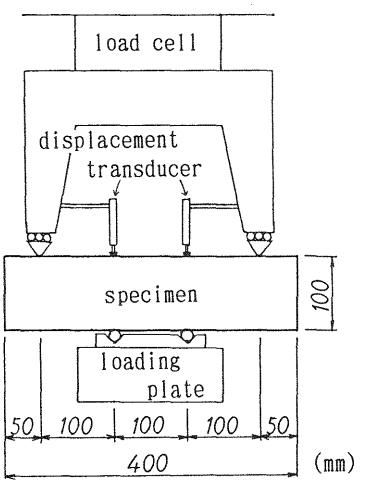

Fig. 2. Setup for four-point bending test

During loading, the surface of concrete specimen is intermittently wiped with ethyl alcohol in order to observe plural cracks which can't be optically observed under normal conditions.

3 Experimental results

3.1 Uniaxial tension test

The behavior after peak load could not be obtained from our experiments; however, four out of six specimens failed at the central part of the 80 x 80 mm cross-section. The probability of occurrence of this phenomenon is generally low. The reasons for the higher occurrence in our tests seem to be the selection of the specimen's form and the effect of the steel leaves. Mean values of maximum load and tensile stress from the four tests were 20.2 kN and 3.2 N/mm^2, respectively.

Fig. 3 indicates load-time relationship and tensile strain-time relationship in each strain gage (s1-s4, in Fig. 4) in specimen T5. Fig. 4 shows the final macrocrack pattern in T5. The loading of T5 is divided into three parts (A, B and C) as shown in Fig. 3. Section A indicates loading-control at the rate of 0.05 kN/s. B and C indicate strain-control at the rate of 0.1 x 10^{-6} 1/s and 0.15 x 10^{-6} 1/s using gage s1. The reason for the switch to 0.15 x 10^{-6} 1/s is that 0.1 x 10^{-6} 1/s was too slow to control the actuator of the loading machine

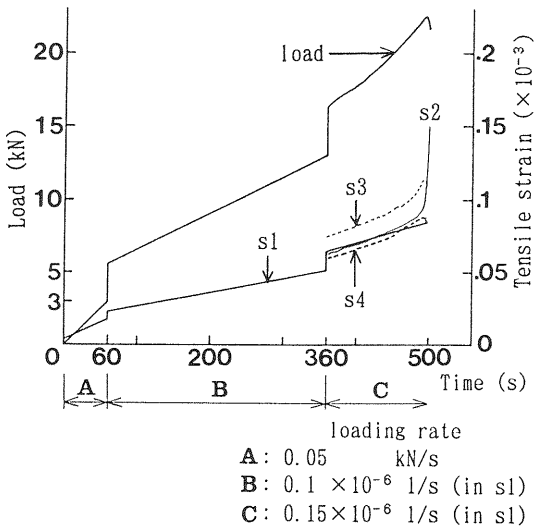

Fig. 3. Load-time and tensile strain-time diagrams (Specimen T5)

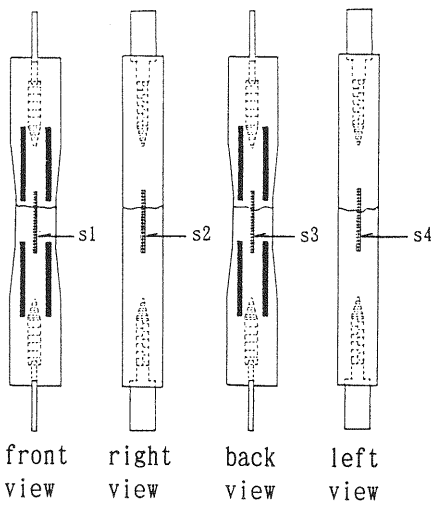

Fig. 4. Macrocrack pattern (Specimen T5)

near the peak load level. However, the T5 test was carried out using the lowest rate of strain of all the tests.

3.2 Four-point bending test

Fig. 5 shows load-displacement relationships above one loading point in the specimen B1-B4. The mean value of peak load was 15.5 kN. Hollow and filled circles in Fig. 5 indicate pauses to change the displacement rate from 0.2×10^{-6} m/s to 0.5×10^{-6} m/s and to observe cracks, respectively. In specimen B2 only, the rate was changed before peak load and plural cracks were observed as shown by the photograph in Fig. 6. This photo was taken at a

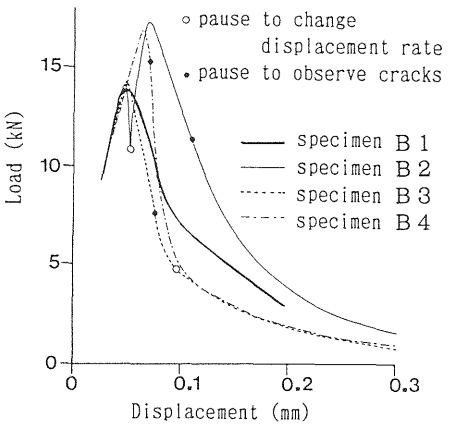

Fig. 5. Load-displacement diagrams

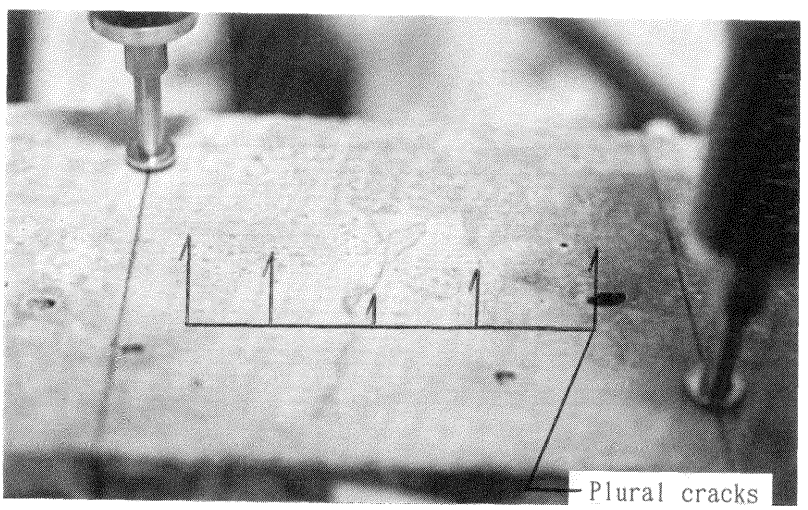

Fig. 6. Photograph of observed plural cracks (Specimen B2)

load of about 14 kN (between the hollow circle and the peak load) and indicates that the crack spacing is about 20 mm. After the peak load all cracks, except the macrocrack located at the center of the photo, were closed and could not be observed even using ethyl alcohol.

4 Analytical model of plural cracks

The developments of plural cracks were analyzed with FEM using a fictitious crack model on an unnotched plain concrete beam under bending. Due to the symmetry only half the beam tested in section 3.2 is considered, as shown in Fig. 7, and isoparametric elements are adopted. Properties of concrete used in this analysis are those given in section 2.1 and a value for Poisson's ratio of 0.2 is adopted. A bilinear 1/10 model is used as the tension softening curve in the fictitious crack model, and the break point is a crack opening displacement of GF/ft. This model was determined by comparing the experimental load-displacement curves in Fig. 5 with the curve obtained from analysis. A GF value of 140 N/m was assumed, taking account of the maximum load values in Fig. 5. Plural cracks are assumed to develop at boundaries of elements in the vertical planes.

A flow chart for determining the position and depth of fictitious cracks is presented in Fig. 8. The fictitious crack tip, at the center of the beam assumed to be a break plane, is increased by each 5 mm (corresponding to one element length). Recognizing that each step is an independent phenomenon in this analysis, the residual strain after crack closure is not taken into consideration.

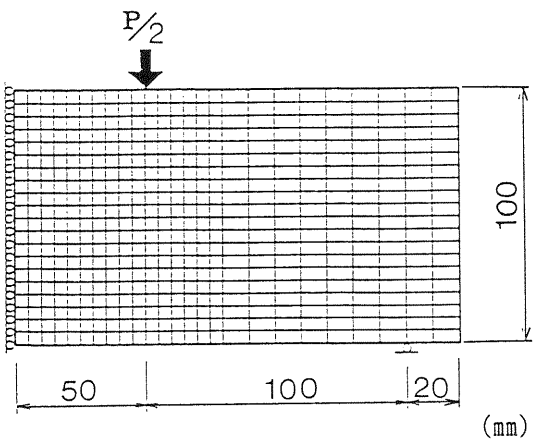

Fig. 7. Element mesh of beam

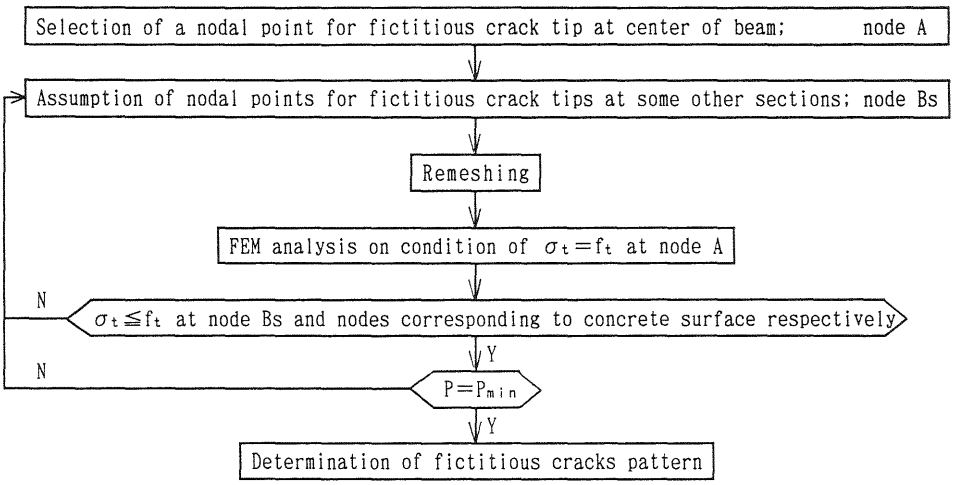

Fig. 8. Flow chart for determining the position and depth of fictitious cracks

5 Analytical results on plural cracks

The simulation result on developments of plural fictitious cracks is shown in Fig. 9. Vertical lines in Fig. 9 indicate the position of fictitious cracks and the depth from the concrete surface to the fictitious crack tips. At P=12.4 kN (prior to obtaining peak load level), it is recognized that some cracks, which exist at P=11.4 kN, are closed. It seems that this phenomenon indicates an interaction of plural cracks. After the peak load of P=14.7 kN, cracks tend to close except for a single crack at the center of the beam. Comparing Fig. 9 with Fig. 6, it is estimated that each of the observed plural cracks in Fig. 6 corresponds to a predicted crack, the depth of which is larger than 20 mm from the surface to the fictitious crack tip.

6 Conclusions

From the work presented in this paper we can draw the following conclusions:

1. In order to cause failure in the central section, the form of the specimen and steel leaves used in this study are effective in uniaxial tension tests of unnotched plain concrete. However, it may be necessary to shorten the specimen length in order to obtain a tension

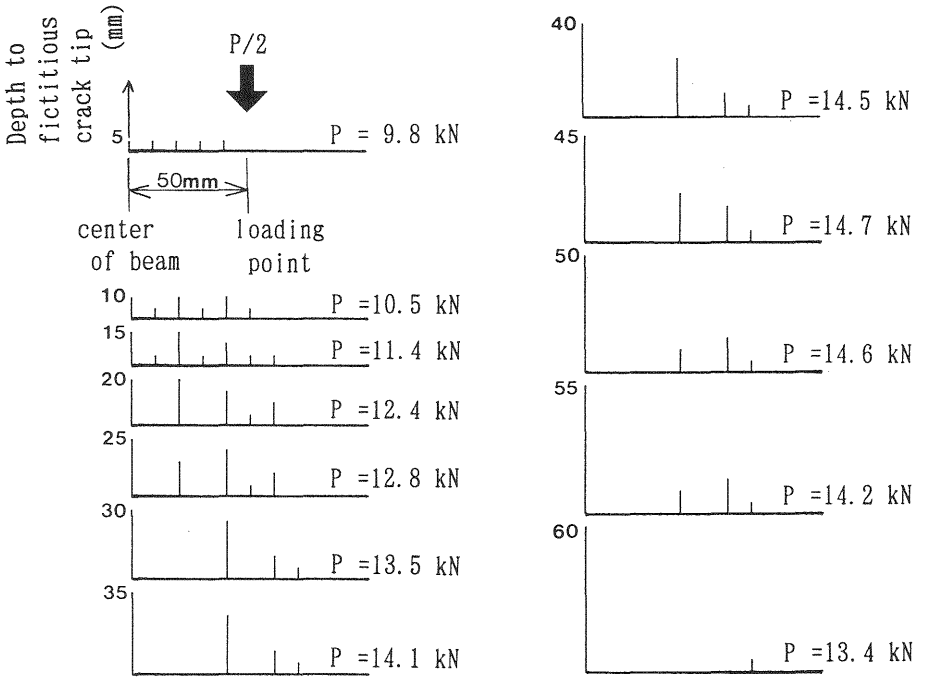

Fig. 9. Simulation result on developments of plural fictitious cracks

softening curve, after giving due consideration to the characteristic length.

2. In four-point bending of unnotched plain concrete beams, comparison of experimental and analytical results indicate that a 1/10 model fits well as a tension softening curve.
3. The behavior of interaction of plural cracks was observed and predicted through experiments and analysis. When a main crack is developing, closing of some cracks occurs.
4. An optical observation of plural cracks is possible by wiping ethyl alcohol onto the concrete surface during loading.
5. From the simulation results, it is indicated that each of the plural cracks observed by the above method corresponds to a predicted crack, the depth of which is larger than 20 mm from the concrete surface to the fictitious crack tip.

7 References

Akita, H., Tomon, M., Koide, H. and Ozaka, Y. (1992) Numerical analysis of three types of cracks in concrete. **Proceedings of Symposium on Computational Methods in Structural Engineering and Related Fields**, 16, 7-12.

Akita, H., Tomon, M., Koide, H. and Takahasi, M. (1993) Analysis of bending fracture of concrete beams by applying several fictitious cracks. **Proceedings of Symposium on Computational Methods in Structural Engineering and Related Fields**, 17, 265-270.

Bazant, Z.P. and Ohtsubo, H. (1977) Stability conditions for propagation of a system of cracks in a brittle solid. **Mechanics Research Communications**, 4, No.5, 353-366.

Hillerborg, A., Modeer, M. and Petersson, P.E. (1976) Analysis of crack formation and crack growth in concrete by means of fracture mechanics and finite elements. **Cement and Concrete Research**, 6, 773-782.

Kurihara, N., Ando, T., Uchida, Y. and Rokugo, K. (1994) Plural cracks of concrete beams in bending. **Proceedings of the Japan Concrete Institute**, 16, No.2, 27-32.

Li, Z. and Shah, S.P. (1994) Localization of microcracking in concrete under uniaxial tension. **ACI Materials Journal**, 91, No.4, 372-381.

Petersson, P.E. (1981) **Crack Growth and Development of Fracture Zones in Plain Concrete and Similar Materials**. Report TVBM-1006, Division of Building Materials, Lund Institute of Technology, Sweden.